Journal of Vegetation Science 15: 711-720, 2004

Remote sensing of protected areas to derive baseline vegetation functioning characteristics

Garbulsky, Martín F.[1*] **& Paruelo, José M.**[2]

[1]*IFEVA - Facultad de Agronomía, Universidad de Buenos Aires - CONICET, Departamento de Producción Animal;*
[2]*Departamento de Recursos Naturales y Ambiente, Av. San Martín 4453, C1417DSE, Buenos Aires, Argentina;*
*E-mail paruelo@ifeva.edu.ar; *Corresponding author; Fax +541145148730; E-mail garbulsky@ifeva.edu.ar*

Abstract

Question: How can we derive baseline/reference situations to evaluate the impact of global change on terrestrial ecosystem functioning?

Location: Main biomes (steppes to rain forests) of Argentina.

Methods: We used AVHRR/NOAA satellite data to characterize vegetation functioning. We used the seasonal dynamics of the Normalized Difference Vegetation Index (*NDVI*), a linear estimator of the fraction of the photosynthetic active radiation intercepted by vegetation (f_{PAR}), and the surface temperature (*Ts*), for the period 1981-1993. We extracted the following indices: *NDVI* integral (*NDVI*-I), *NDVI* relative range (R_{rel}), *NDVI* maximum value (V_{max}), date of maximum *NDVI* (D_{max}) and actual evapotranspiration.

Results: f_{PAR} varied from 2 to 80%, in relation to changes in net primary production (*NPP*) from 83 to 1700 $g.m^{-2}.yr^{-1}$. *NDVI*-I, Vmax and f_{PAR} had positive, curvilinear relationships to mean annual precipitation (*MAP*), *NPP* was linearly related to *MAP*. Tropical and subtropical biomes had a significantly lower seasonality (R_{rel}) than temperate ones. D_{max} was not correlated with the defined environmental gradients. Evapotranspiration ranged from 100 to 1100 $mm.yr^{-1}$. Interannual variability of *NDVI* attributes varied across the temperature and precipitation gradients.

Conclusions: Our results may be used to represent baseline conditions in evaluating the impact of land use changes across environmental gradients. The relationships between functional attributes and environmental variables provide a way to extrapolate ecological patterns from protected areas across modified habitats and to generate maps of ecosystem functioning.

Keywords: Argentina; Biome; Evapotranspiration; NOAA/AVHRR; NDVI; NPP; Surface temperature.

Abbreviations: CV = Coefficient of variation; D_{max} = Date of maximum NDVI; *e* = Light use efficiency; *Et* = Evapotranspiration; f_{PAR} = Fraction of photosynthetic active radiation intercepted by vegetation; *MAP* = Mean annual precipitation; *MAT* = Mean annual air temperature; *NDVI* = Normalized difference vegetation index; NDVI-I = NDVI integral; *NPP* = Net primary production; PAL = Pathfinder AVHRR Land; *PUE* = Precipitation use efficiency; R_{rel} = NDVI relative range; *Ts* = Surface temperature; V_{max} = *NDVI* maximum value

Introduction

Identification of the effects of climatic change, desertification or land use requires characterization of the baseline structure and function of vegetation, including patterns of spatial and temporal variation. Describing the structure and functioning of the original vegetation (prior to human influence, potential vegetation in the sense of Tüxen 1956) and its temporal and spatial variability imposes a serious challenge. The most common way to describe the original vegetation is by interpolating or extrapolating data from point observations of undisturbed areas. Such spatial generalizations may be based on models of the relationship between plant attributes and climatic variables (Prentice et al. 1992; Paruelo et al. 1998). In general, the description of the original vegetation is based only on structural attributes of the vegetation such as physiognomy, dominant species, plant functional types proportions or total cover (Stephenson 1990; Leemans & van der Born 1994).

Vegetation functioning, the exchange of matter and energy with the environment, is often characterized by net primary production (*NPP*). Many functional characteristics, such as biomass consumption by herbivores (Oesterheld et al. 1992) and net nitrogen mineralization (Burke et al. 1997) are highly correlated with primary production. *NPP* is then an integrative descriptor of ecosystem functioning (McNaughton et al. 1989). *NPP* is strongly dependent on the amount of absorbed radiation and water availability. Monteith (1981) presented a simple model where *NPP* is a linear function of the annual integral of absorbed photosynthetic active radiation (APAR). Water availability is the main control of the amount of radiation absorbed by the canopy and hence the major determinant of *NPP* in deserts, grasslands and savannas (Noy Meir 1973; Sala et al. 1988).

In spite of its significance, finding comparable *NPP* data for a wide diversity of biomes is difficult. Moreover, mean or one year values are insufficient; baseline conditions should be characterized from a long-term database to identify temporal trends in vegetation

attributes. Seasonal and interannual variability of vegetation functioning are both important time frames to understand the variability of CO_2 exchanges between biosphere and atmosphere (Potter et al. 1999). Remotely sensed data provide information that could be related to photosynthesis and water fluxes. The fraction of the photosynthetic active radiation absorbed by the canopy (f_{PAR}) and hence primary productivity (Box et al. 1989) and evapotranspiration (*Et*) (Running & Nemani 1988; Di Bella et al. 2000) can be estimated from satellite data.

Our goal was to implement an approach to characterize relatively undisturbed areas across environmental gradients. Protected areas usually include ecosystems little modified by human activities. We use, as an example, the National System of Protected Areas (SNAP) of Argentina, which ranks first in the southern hemisphere in the diversity of biomes represented, the range of climates incorporated and the quality of protection provided (Anon. 1992). We show that protected areas provide a unique opportunity for deriving baseline/reference situations to evaluate the impact of global change on terrestrial ecosystems. Moreover, functional ecosystem attributes measured through remote sensing techniques can provide a 'common currency' for definition of reference conditions across geographical regions.

Our specific objectives were to analyse functional attributes related to the energy flow (light absorption), water dynamics (evapotranspiration) and the interannual variability of such variables across a broad geographical region (22° - 54° S). We describe also the range of *NPP* associated with different biomes derived through published light use conversion efficiency coefficients. We were especially interested in deriving empirical relationships between ecosystem functional attributes and their variability across environmental gradients. Such empirical models permit generalization about potential functioning of the vegetation over extensive areas.

Material and Methods

We used Normalized Difference Vegetation Index (*NDVI*) and surface temperature (*Ts*) data derived from the Pathfinder AVHRR Land (PAL) database to characterize the vegetation functioning of 13 protected areas in Argentina (Fig. 1). These spectrally derived variables were surrogates for f_{PAR} and actual *Et*. From f_{PAR} we calculated *NPP*.

The analysis encompasses vegetation extending across gradients of mean annual precipitation from 50 to 1700 mm and mean annual temperature from 5 to 25 °C. We geo-referenced all protected areas included in the national system larger than 470 km^2 on Landsat TM images and on topographic maps (scale 1 : 250 000; Instituto Geográfico Militar, Argentina). Because of these criteria, some important biomes, such as the Pampas grasslands and the Patagonian steppes, were not included in our analyses.

The PAL images have a spatial resolution of 8 km × 8 km (James & Kalluri 1994, ftp://daac.gsfc.nasa.gov/data/avhrr/). The database included 432 10-day composite images, covering the period July 1981 to June 1993. *NDVI* was calculated as $(ch_2 - ch_1)/(ch_2+ch_1)$, where ch_1 and ch_2 are the reflectance in channel 1 (0.58-0.61 μm) and channel 2 (0.725-1.1 μm) measured by the AVHRR sensor. *Ts* was calculated from channel 4 (10.3-11.3 μm) and corrected by the surface emissivity using *NDVI* and channel 5 (11.5-12.5 μm) (Sobrino et al. 1991). To minimize the effect of errors associated with sensor degradation, sensor angle and atmospheric contamination not removed by prior processing, we corrected each raw *NDVI* value using the *NDVI* of the Atacama desert (23° S - 69° W), in northern Chile, assuming constant and null *NDVI* for this region (Kaufman & Holben 1993); any temporal variation in *NDVI* of the Atacama desert was assumed to be noise. Then: $NDVI_i$-corrected = $NDVI_i$-raw – $NDVI_i$- Atacama, where *i* represents the image number from 1 to 432. Negative values were discarded and the entire database was filtered for inconsistent values. Viovy et al. (1992) showed that a rate of change of *NDVI* of 2% per day lacks biological significance for natural vegetation. Suspect values were replaced by more representative ones recorded previously or immediately following. The use of the maximum or the mean value of the previous and the following values to replace the suspect values did not alter the general patterns presented. Each protected area was characterized for each date by the mean of *NDVI* and *Ts* of four pixels entirely included in the area. For areas including more than four pixels a random selection was performed among pixels completely included in the main vegetation type of the protected area.

For each pixel we derived four annual attributes from the *NDVI* curves: the annual *NDVI* integral (*NDVI*-I), the maximum *NDVI* (V_{max}), the date of the maximum *NDVI* (D_{max}) and the relative range (R_{rel}). *NDVI*-I is an estimator of f_{PAR} (Tucker & Sellers 1986) and is the annual *NDVI* mean from July to June. R_{rel} is an estimator of the seasonality of the light absorption – (V_{max}– Min *NDVI*)/*NDVI*-I. We also characterized the interannual variability of each attribute using the coefficient of variation over the 13 years of the study (CV% = standard deviation/mean × 100).

To assess the spatial and interannual variability of latent heat exchange between the vegetation and the atmosphere, we applied a simple correlative model to estimate actual *Et* from remotely sensed data. We

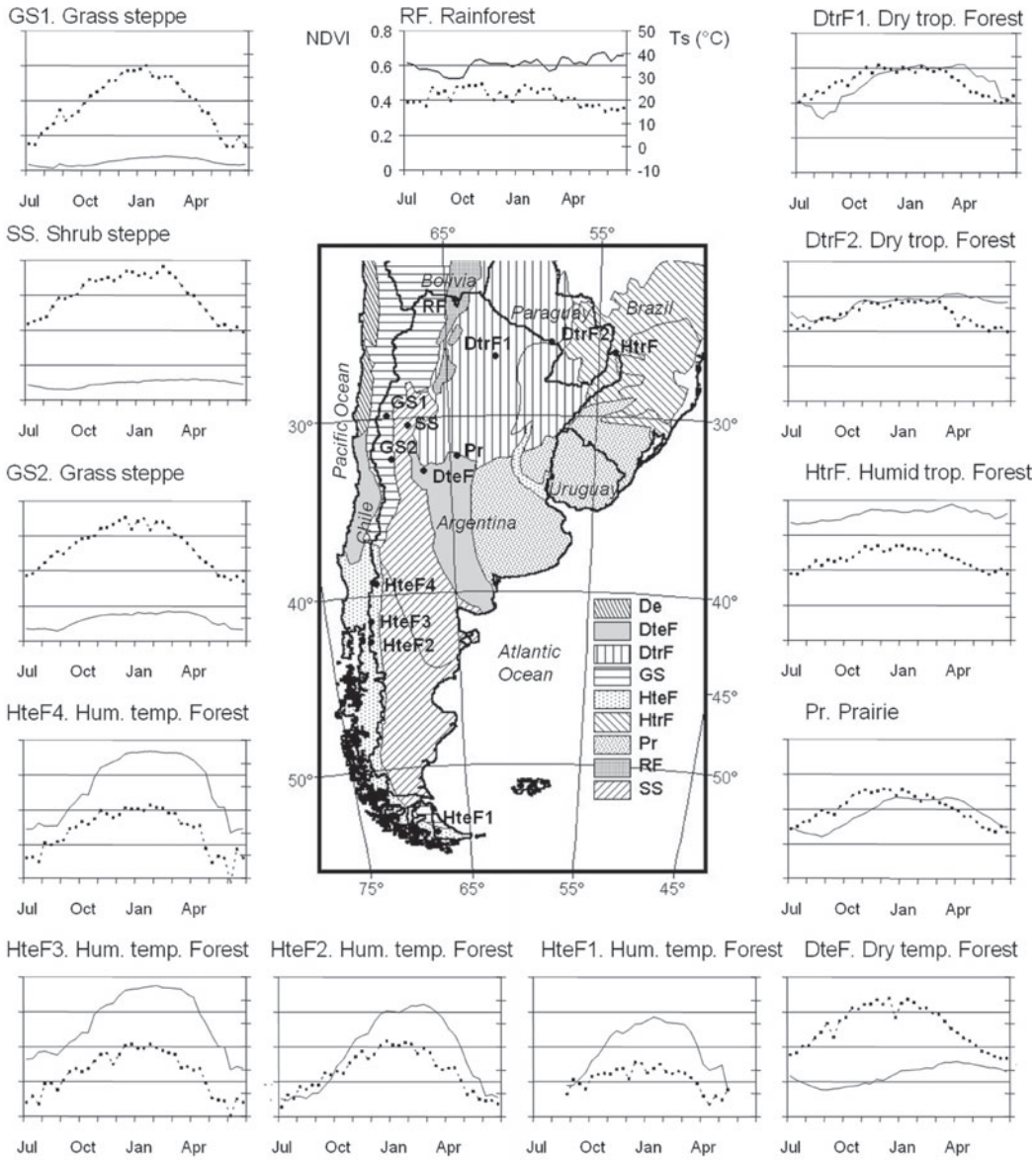

Fig. 1. Protected areas included in the analysis. Marginal plots show the dynamics of mean values of *NDVI* — and *Ts* - - - over 12 yr (1981-93) and four pixels (4 × 64 km^2). Left axis corresponds to *NDVI* and right axis to *Ts* (°C). Shaded areas indicate the main biomes of southern South America (after Hueck & Seibert 1981): deserts (De), dry temperate forests (DteF), dry tropical forests (DtrF), grass steppes (GS), humid temperate forests (HteF), humid tropical forests (HtrF), prairies (Pr), rainforest (RF), and shrub steppes (SS). See Apps. 1-3 for detailed descriptions of protected areas.

calculated mean monthly *Et* from mean meteorological data (Anon. 1985) for ten of the study areas for which appropriate data were available. Potential *Et* (Anon. 1985) was calculated using Penman's equation (Allen et al. 1988). To calculate actual *Et* we used the following decision rules:

$$etp_i \geq pp_i + stw_{i-1} \Rightarrow etr_i = pp_i + stw_{i-1}$$
$$etp_i < pp_i \Rightarrow etr_i = etp_i \quad (1)$$

where etp_i is monthly potential evapotranspiration, pp_i is monthly precipitation, stw_i is the water storage in the soil and etr_i is actual evapotranspiration.

A model that uses soil texture (derived from a national soil database; Anon. 1990) was used to estimate soil water holding capacity (*whc*, Saxton et al. 1986). Soil water storage ranged between 68 and 416 mm. Because of differences in the grain of the soil maps and the PAL data, it was impossible to assign a *whc* to each pixel. We then assumed a uniform *whc* close to the mode of the different soils included in the

study. A sensitivity analysis showed negligible effects of *whc* on the model fitted at regional scales. The PAL remotely sensed variables included in the model were mean monthly *Ts* and *NDVI*. June to August data for humid temperate forests (54° S) were discarded because of the lack of reliable satellite data during winter months.

We evaluated linear regression models, using a stepwise procedure (Anon. 1996), including *Ts* and *NDVI*, their logarithmic and exponential transformations and their interaction (*Ts*NDVI*) as independent variables, and etr_i as dependent variable. We also calculated actual evapotranspiration from the correlative model proposed by Di Bella et al. (2000). We evaluated our model by comparing the annual *etr* estimates for a random set of 28 climatic stations from FAO (Anon. 1985) in unprotected areas. We tested (*F*-test) whether the regression line differs from the 1 : 1 line. The use of only *Ts* and *NDVI* to estimate *etr* is clearly a simplification (although widely used; Moran et al. 1994) because it does not include all the terms of the energy balance of a surface (net radiation and wind).

To translate our comparative index of carbon gains (*NDVI*-I) into a biological meaningful variable, we calculated *NPP* from remotely sensed data using the model proposed by Monteith (1981).

$$NPP\ [\text{g-dry-matter.m}^{-2}.\text{yr}^{-1}) = e * PAR * f_{PAR} \quad (2)$$

Where e = light use efficiency (a coefficient of conversion of absorbed light into total dry matter) and PAR the incoming photosynthetically active radiation derived from FAO (Anon. 1985). f_{PAR} was estimated from *NDVI* by linear interpolation between the *NDVI* corresponding to areas with zero light absorption (Atacama desert, 69° W, 23° S) and near 100% of light absorption (Amazonian rainforest, 69° W, 10° S). The values of e for each vegetation type were obtained from Field et al. (1995) and converted to dry matter assuming a carbon to dry matter ratio of 0.475 (0.595 (g-dry-matter.MJ^{-1}] for Humid Temperate forest, 0.745 for Rain forest/Humid Subtropical forest, 0.635 for Dry forest, 0.437 for Shrub steppes and 0.629 for Grassland/grass steppe). Regrettably, no data are available to evaluate the NPP estimates generated across such a wide environmental gradient.

Results

NDVI and *Ts* provided good estimates of monthly actual evapotranspiration as calculated from meteorological data (etr_{met}). The best model fitted at the regional scale is ($r^2 = 0.84$; $n = 113$; $p < 0.0001$):

$$etr_{met}\ (\text{mm/month}) = Ts * NDVI * 5.57 \quad (3)$$

To test the stability of the general model (2), we constructed an independent model for each protected area (Table 1). Annual mean surface temperature for A particular site (Ts_{avg}) accounted for 65% of the regional variability of the slope of the relationship (Slope = 23.11 – 12.41 logTs_{avg}; $n = 10$, $p = 0.0049$). Thus, the general evapotranspiration model can be rewritten as:

$$etr_{met}\ (\text{mm.mo}^{-1}) = Ts * NDVI * [23.11 - 12.41 \log (Ts_{avg})] \quad (4)$$

The evaluation of the general model showed that *etr* estimates derived from meteorological and remotely sensed (etr_{sat}) data were highly correlated ($etr_{met} = 1.02$; etr_{sat} - 88.20; $r^2 = 0.82$; $n = 28$; $F = 132.8$; $p < 0.0001$) and did not differ from the 1 : 1 line (*F*-test, $F = 0{,}005$, $p > 0.8$, df = 52).

Seasonal trajectories in the *NDVI-Ts* space varied with vegetation type from linear to cyclic patterns (Figs. 1 and 2a). We quantified the trajectory by the coefficient of determination (r^2). Coupling of seasonal dynamics of *NDVI* and *Ts* was highest in temperate forests, intermediate in subtropical forest and grassland ecosystems and lacking in shrub steppes. In general, forests present lower slopes than the steppes. Only one site (RF, in

Table 1. Slope and coefficient of determination (r^2) of the models of the relationship between monthly *etr* and *Ts*.*NDVI* for each protected area and for all the sites. The slope (± SE) and the coefficient of determination for each site indicate the parameter for the model of the same form as the general (*etr* = *a*.*Ts*.*NDVI*). In every case the models were significant ($p < 0.001$). * denotes slopes statistically different from the slope of the general model, tested by an *F* hypothesis test. See Fig. 1 for protected area codes.

Protected area	Slope	r^2	*n*
DteF	5.60 ± 1.04	0.69	12
DtrF1	*3.88± 0.52	0.81	12
DtrF2	*7.42 ± 0.39	0.96	12
GS1	*11.03 ± 1.45	0.82	12
GS2	*1.80 ± 0.21	0.85	12
HteF1	*15.08 ± 1.93	0.88	8
HteF3	7.91 ± 1.04	0.82	9
HtrF	4.88 ± 0.38	0.93	12
Pr	5.88 ± 0.53	0.90	12
SS	5.04 ± 0.86	0.73	12
All the sites	5.57 ± 0.24	0.84	113

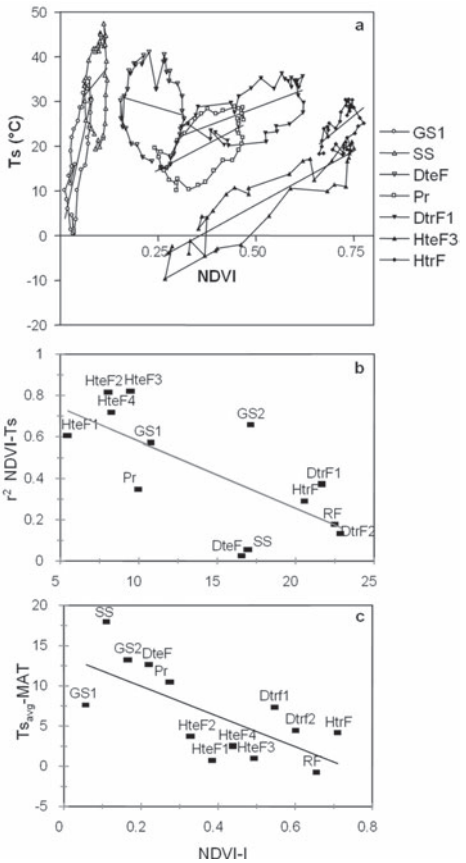

Fig. 2a. Seasonal trajectories of the 1981-1993 mean 10-day *NDVI* and *Ts* for seven selected sites and the corresponding regression lines. **b.** Regional relationship between the strength of *NDVI-Ts* relationships (coefficient of determination of the *NDVI-Ts* relationship) and *MAT* for the 13 protected areas: $r^2_{(NDVI-Ts)} = 0.90 - 0.032MAT$; $r^2 = 0.55$; $p < 0.01$). **c.** Difference between mean Ts_{avg} and *MAT* along the *NDVI*-I regional gradient:
$Ts_{avg} - MAT = 13.73 - 18.81NDVI\text{-I}$; $r^2 = 0.49$; $p < 0.01$).

tropical forest) presented a significant negative relationship. We detected an inverse relationship between the strength of the seasonal coupling between *NDVI* and *Ts* and mean annual air temperature (*MAT*). *MAT* accounted for 55% of the regional variability in r^2 (Fig. 2b), with warm areas showing least coupling of dynamics of *NDVI* and *Ts*. The *NDVI*-I accounted for 49% of the regional variability in the difference between Ts_{avg} and *MAT* (Fig. 2c).

Mean annual precipitation (*MAP*) was positively associated with *NDVI*-I and V_{max} (Fig. 3a, c). A saturation function best described the relationships, with R_{rel} lowest at high *MAP* (Fig. 3b). *MAT* accounted for 78% of the regional variability in R_{rel} (Fig. 3e). Regional patterns of the other attributes were not significantly associated with the temperature gradient (Fig. 3d, f). D_{max} did not have a significant relationship with *MAP* or *MAT*.

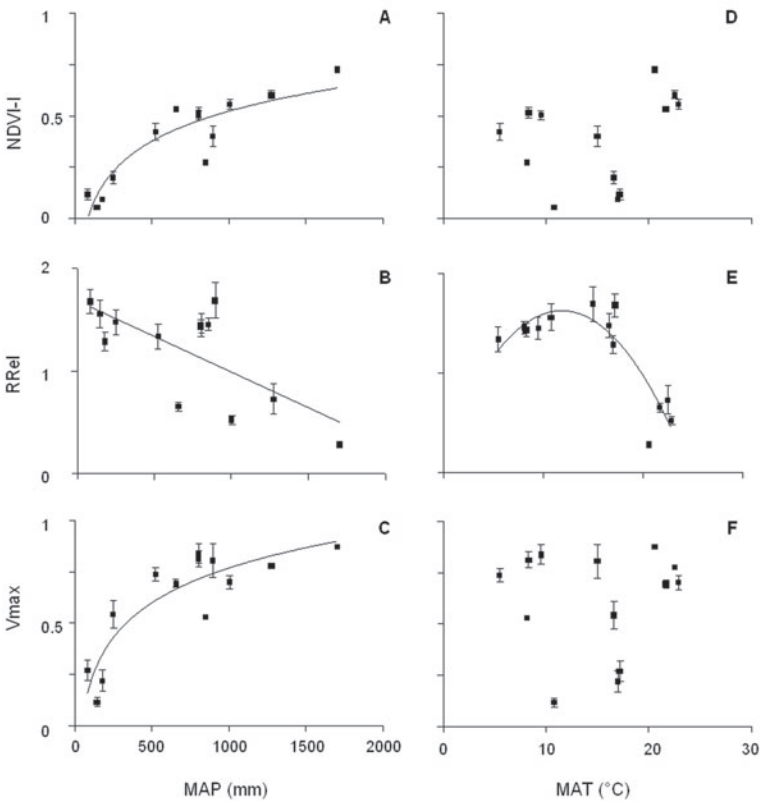

Fig. 3. Relationship between climatic gradients (*MAP* and *MAT*) and *NDVI* attributes of 13 protected areas of Argentina for the 1981-1993 period. Error bars show SD for four pixels per site. **A.** and **D.** *NDVI*-I; **B**. and **E**. R_{rel}; **C**. and **F**. V_{max}. Linear regression lines are significant, $p < 0.01$.
A. $NDVI\text{-I} = -0.93 + 0.48 \log MAP$, $r^2 = 0.81$;
B. $R_{rel} = -0.00069.MAP + 1.68$, $r^2 = 0.48$;
C. $V_{max} = -0.91 + 0.56 \log MAP$, $r^2 = 0.78$;
E. $R_{rel} = 0.248 + 0.232.MAT - 0.0097.MAT^2$, $r^2 = 0.78$.

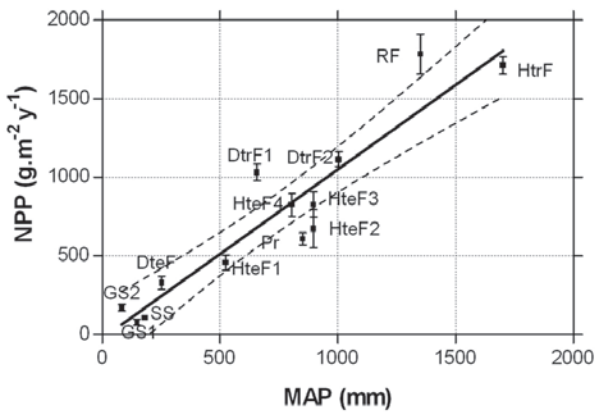

Fig. 4. *NPP* of protected areas in Argentina as estimated from remotely sensed data. Mean annual values for the 13 protected areas are plotted against *MAP*, $n = 13$; $r^2 = 0.87$; $p < 0.0001$.
NPP (g-dry-matter.m^{-2}.yr^{-1}) = –25.33 + 1.076 *MAP* (mm). Solid line shows the best fit and dotted line 95% confidence intervals. Error bars show SD for 12 growing seasons.

Estimated *NPP* ranged from 83 g-dry-matter.m^{-2}.yr^{-1} in grass steppes to more than 1700 in rainforest (Fig. 4). A fitted linear model was significant for *NPP* along the *MAP* gradient for all the sites. The mean precipitation use efficiency (*PUE*), defined as the slope of the regional regression between *NPP* and *MAP*, was 1.076 g-dry-matter.m^{-2}.mm^{-1}. The ineffective precipitation (i.e. the *X*-intercept; Sala et al. 1988) was 23.55 mm.yr^{-1}.

Mean annual actual etr_{sat} increased from a grass steppe site (< 100 mm.yr^{-1}) to a tropical forest site (> 1100 mm.yr^{-1}, Fig. 5a). etr_{sat} was positively correlated with *MAP* (Fig. 5a) and *MAT* (Fig. 5d). Maximum monthly evapotranspiration was positively correlated with *MAP* (Fig. 5c). etr_{sat} seasonality was negatively correlated with *MAT* (Fig. 5e) and unrelated to *MAP* (Fig. 5b).

We found a strong negative relationship between precipitation and the coefficient of variation of *NDVI*-I (Fig. 6a). CV *NDVI*-I decreased from shrub steppes (SS, 20%) to humid tropical forest (HtrF, 2%). CV R_{rel} was, in general, higher than CV *NDVI*-I (Fig. 6a, b). V_{max} and *NDVI*-I were both negatively correlated with precipitation across years (Fig. 6c). CV V_{max} was lower than the CV *NDVI*-I for all sites. The interannual variability of *NDVI*-I and V_{max} was best fitted by an optimum function change along the *MAT* gradient (Fig. 6d, f). *MAT* positively accounted for the interannual variability of the R_{rel} (Fig. 6e) and D_{max}. No clear patterns of change in the coefficient of variation of *etr* were detected across *MAP* or *MAT* gradients.

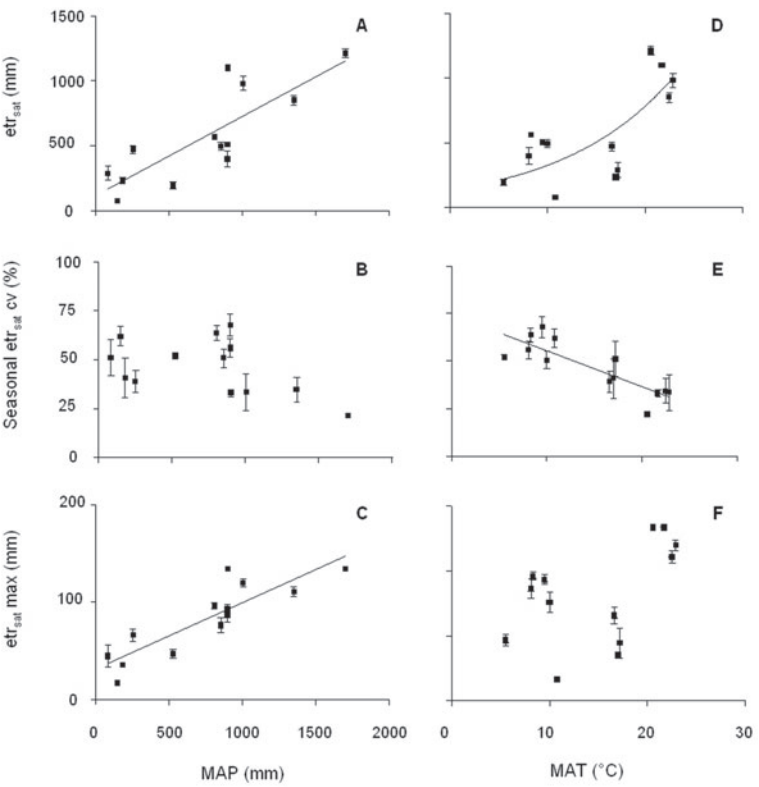

Fig. 5. Relationship between climatic gradients (*MAP* and *MAT*) and etr_{sat} attributes of 13 protected areas in Argentina for the 1981-1993 period. Error bars show s.d. for four pixels per site.
A. and **D**. etr_{sat}; **B**. and **E**. Seasonal coefficient of variation; **C.** and **F.** Maximum evapotranspiration. Regression lines are significant, $p < 0.01$.
A. etr_{sat} (mm) = 117 + 0.32. *MAP*, $r^2 = 0.67$;
C. Max. monthly etr_{sat} (mm) = 31.4 + 0.068. *MAP*, $r^2 = 0.76$;
D. etr_{sat} (mm) = 132.2.e$^{(0.087.MAT)}$, $r^2 = 0.55$;
E. $R_{rel} = 74.25 - 1.89.MAT$, $r^2 = 0.70$.

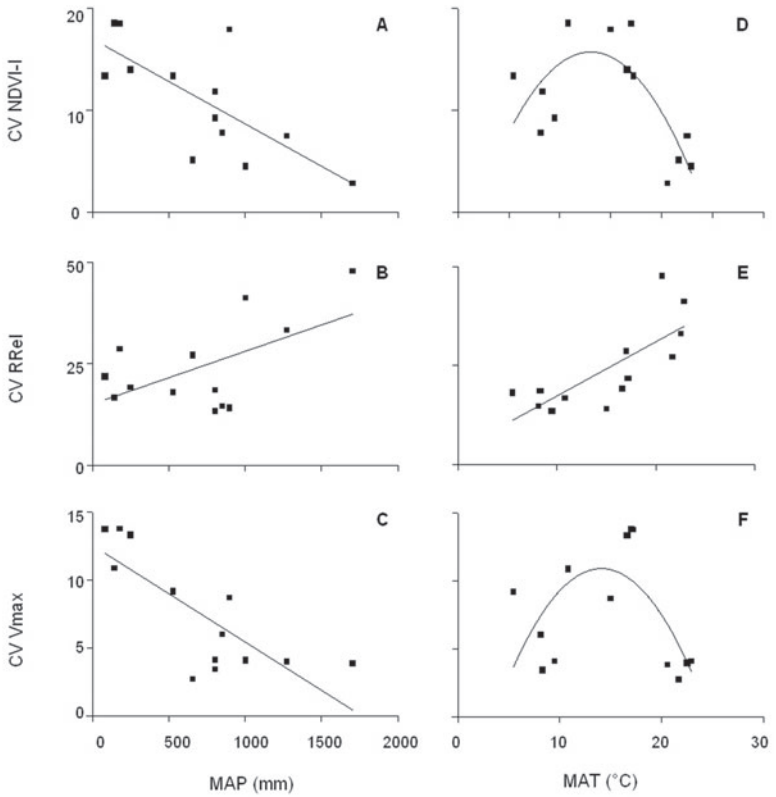

Fig. 6. Relationship between climatic gradients (*MAP* and *MAT*) and *NDVI* attributes of 13 protected areas in Argentina for the 1981-1993 period. Error bars show s.d. for four pixels per site. **A.** and **D.** Coefficient of variation of *NDVI*-I; **B.** and **E.** CV of R_{rel}); **C.** and **F.** Coefficient of variation of V_{max}.
A. CV *NDVI*-I = 17.01 – 0.0083.*MAP*;
$r^2 = 0.53$; $p < 0.01$.
B. CV R_{rel} = 15.09 + 0.013.*MAP*;
$r^2 = 0.32$; $p < 0.05$.
C. CV V_{max} = 12.59 – 0.0071.*MAP*;
$r^2 = 0.62$; $p < 0.01$.
D. CV *NDVI*-I = –5.1 + 3.19.*MAT* – 0.12 MAT^2;
$r^2 = 0.55$; $p < 0.1$.
E. CV R_{rel} = 3.6 + 1.37.*MAT*;
$r^2 = 0.58$; $p < 0.01$.
F. CV V_{max} = –8.4 + 2.75.*MAT* – 0.09 MAT^2;
$r^2 = 0.40$; $p < 0.01$.

Discussion

Our approach, based on a regional analysis of protected areas and functional attributes, provided a description of how ecosystem functioning and its variability change across environmental gradients under minimum human alteration. Despite the differences in vegetation structure and seasonality among the sites, *MAP* was a good estimator of *NDVI*-I, a descriptor of light absorbed by the canopy. The relationship between *MAP* and both *NDVI*-I and V_{max} across the analysed gradient showed a saturation type form (Fig. 3a). Previous studies showed this type of relationship between *NDVI*-I and *MAP* (Box et al. 1989; Paruelo & Lauenroth 1995). The linear relationship between *NPP* and *MAP* may arise from the differences in incoming radiation and light use efficiency among sites. Differences in the relationships of *NDVI*-I and *NPP* with *MAP* for some areas could be a consequence of the intrinsic capacity of each biome to transform radiation into biomass as well as the differences in incoming PAR among sites.

Few field based estimates of *NPP* field data are available for South American biomes. Most studies recorded only above-ground NPP in grasslands and shrublands (e.g. Pucheta et al. 1998). Moreover, none of this information comes from protected areas and only part of it covers more than one year. For forest ecosystems, data are even scarcer. For *Nothofagus* temperate forests in Argentina and Chile, fine litter production (Veblen et al. 1996) had a range of 200 to 740 g-dry-matter.m^{-2}.yr^{-1} from south to north. For a site located 200 km south of site HteF2, Austin & Sala (2002) showed a fine litter production of the tree canopy of 315 g-dry-matter.m^{-2}.yr^{-1}. This figure may represent 70% of *NPP* above-ground (Austin pers. comm.) because wood increment and understorey production were not considered. We did not find data for the other forest ecosystems.

NPP estimates based on Monteith's equation (1981) are highly dependent on *e*-values. Many uncertainties still remain in estimates of *e* for different biomes (Goetz & Prince 1999). The use of Monteith's equation, however, circumvents some difficulties with other models. We were not able to use alternative models to estimate *NPP* from remotely sensed data (e.g. Coops & Waring 2001) because they were biome specific, or dependent on detailed meteorological data that we lacked for the full data set.

Our estimates of *NPP* were not evaluated against field data, so they may be most useful as indicators of trends in carbon gains across the main environment gradient. However, the parameters of the *NPP-MAP* relationship had a good correspondence with previous studies. The slope of the above-ground *NPP-MAP*

relationship, *PUE*, ranged between 0.26 to 0.85 g-dry-matter.m^{-2}.mm^{-1} (McNaughton et al. 1993). For South American sites distributed across a mean annual precipitation gradient from 100 to 1400 mm, the above-ground *NPP-PUE* was 0.48 g-dry-matter.m^{-2}.mm^{-1} (McNaughton et al. 1993). Our results for *NPP* had a slope twofold higher than that for the above-ground *NPP* data. For shrubland and grassland areas Milchunas & Lauenroth (1992) suggested a ratio for above-ground/below-ground *NPP* between 1.76 and 3.76. Data give a ratio of 0.32 for tropical forests (Wright 1996) and 0.78 for temperate forests (Curtis et al. 2002). Our *X*-intercept was 38 mm below the reported value for above-ground *NPP* in South America. It was, however, in the range reported for other regions of the world (23 -148 mm; Noy Meir 1973, Sala et al. 1988, McNaughton et al. 1993).

MAP was associated with both descriptors of *NPP* dynamics (Fig. 3b, c), but D_{max} had no relationship with environmental variables. This may be due, in part, to the effects of high winter precipitation occurring during vegetation senescence and becoming available only with spring snow melt in colder regions. Site HteF1, the southernmost area considered, consistently had an earlier *NDVI* peak than the other sites. Low temperatures in late summer could initiate senescence, as suggested for an altitudinal gradient (Barrera et al. 2000).

Across the studied biomes, we found a more diverse range of responses of the *NDVI-Ts* trajectories than previously shown for North America (Nemani & Running 1997). A summary of the trajectories of *NDVI-Ts* based on maximum values may not capture fully the heterogeneity of biomes studied here because the approach conceptually ignores biomes with *NDVI-Ts* negative correlations, as we found for one site. Problems with the use of maximum values may be particularly serious for mediterranean climates, where *NDVI* and *Ts* peaks can be highly decoupled (e.g. site DteF). *Ts* peaks earlier than *NDVI* for all of our sites. We suggest that the slope of the *NDVI-Ts* relationship might reflect at least two important functional features of vegetation. First, it reflects the ecosystem-specific functional response to seasonal temperature variations. Vegetation types with high *NDVI*-I values had lower slopes than those with low *NDVI*-I, which suggest that vegetation is buffering effects of temperature increase. Second, we suggest that this slope could be used to evaluate the impact of land use. We hypothesize a wide variety of functional responses for each vegetation type depending on land use change. For instance, the replacement of temperate forest with evergreen trees would increase the slope because of higher minimum *NDVI* value with similar winter temperatures and similar maximum values for *NDVI* and *Ts*. The replacement of a subtropical forest by cropland would reduce the slope because of a decrease of minimum *NDVI* and an increase of minimum *Ts* and similar maximum *NDVI* and *Ts* values.

The coefficient of determination of the *NDVI-Ts* relationship integrates, in part, differences between dynamics of leaf expansion, defined as the period of *NDVI* increase and senescence. High r^2 indicates similar relationships between *NDVI* and *Ts* during leaf expansion and senescence. However, *Ts* was higher during leaf expansion than during senescence for all biomes and *Ts* peaked earlier than *NDVI*, even for rainforest, where *NDVI* and *Ts* were negatively correlated. At a global scale and at a coarse spatial resolution, the correlation between weekly *NDVI* and *Ts* varies with latitude, a surrogate of *MAT* (Schultz & Halpert 1995). Our results support this pattern; additionally, we separate the trajectories of leaf expansion and senescence. We showed that *MAT* accounted for most of the regional variability of the *NDVI-Ts* seasonal relationship.

Characterization of the temporal variability of ecosystem attributes is critical for detection of changes or trends associated with management, degradation or global change. Our analysis not only provides regional estimates of the interannual variability of six functional attributes but also shows relationships of that variability to environmental variables. Other studies have shown decreased seasonal variability of total carbon gains as *MAP* increases (Fig. 6a) (Paruelo & Lauenroth 1998). We showed that V_{max} shows a similar behaviour. However, *NDVI*-I varied more between years than V_{max} (Fig. 6a, c). As noted in other studies (e.g. Paruelo et al. 1999) the coefficient of variation of total carbon gain is lower than the coefficient of variation of precipitation, suggesting that climatic variability is buffered with respect to ecosystem functioning.

The interannual variability of carbon gains and seasonality also varied across the *MAT* gradient. Again, *NDVI*-I and V_{max} had a different response than R_{rel} (Fig. 6d, e, f). We hypothesize that high variability in *NDVI*-I and V_{max} in the middle portion of the gradient is a consequence of variability in water flux, because these sites are also the driest. Our analysis did not include a site in a temperate humid area, such as the Pampas grasslands, because there are no large protected areas in this region.

We present, then, baseline conditions to evaluate the impact of global changes across environmental gradients. We developed, for a broad range of environmental conditions over a large part of South America, quantitative relationships between vegetation functioning and climatic variables. These may be used to extrapolate information gathered on protected areas across human modified areas and to generate maps representing departure from more natural, less modified ecosystems.

This approach may be replicated in different areas to derive quantitative relationships among vegetation traits and climatic variables. Such analysis would not only improve the relationships found but also may describe important contrasts among areas differing in flora, evolutionary history or human impact.

Acknowledgements. This work was founded by the Fundación Antorchas, InterAmerican Institute for Global Change Research (ISP 3-077 and CRN 012), Proyungas, University of Buenos Aires (UBA) and CONICET. This article is a contribution to the 'Plan Estratégico UBA' (15.982/2000 Anexo 33). L. Goveto and M. Mermoz from the Adminstración de Parques Nacionales helped in gathering National Parks information. Data used in this study include data produced through funding from the EOS Pathfinder Program (NASA) in cooperation with NOAA. Data were provided by the EOS Data and Information System, DAAC at Goddard Space Flight Center. K. Woods, R.H. Waring, S. Running, S. Kang, M.R. Aguiar and I. Fabricante provided useful suggestions to improve the manuscript.

References

Anon. 1985. *Datos Agroclimáticos para América Latina y el Caribe*. FAO - Food and Agriculture Organization of the United Nations, Rome, IT.

Anon. 1990. *Atlas de suelos de la República Argentina*. 2 Vols. Instituto Nacional de Tecnología Agropecuaria. Buenos Aires, AR.

Anon. 1992. *Global biodiversity: Status of the Earth's living resources*. World Conservation Monitoring Centre and Chapman & Hall, London, UK.

Anon. 1996. *SAS Release 6.12*. SAS Institute Inc., Cary, NC, US.

Allen, R.G., Pereira, L.S., Raes, D. & Smith, M. 1988. *Crop evapotranspiration – Guidelines for computing crop water requirements – FAO Irrigation and drainage paper 56*. FAO, Rome, IT.

Austin, A.T. & Sala, O.E. 2002. Carbon and nitrogen dynamics across a natural precipitation gradient in Patagonia, Argentina. *J. Veg. Sci.* 13: 351-360.

Barrera, M.D., Frangi, J.L., Richter, L.L., Perdomo, M.H. & Pinedo, L.B. 2000. Structural and functional changes in *Nothofagus pumilio* forests along an altitudinal gradient in Tierra del Fuego, Argentina. *J. Veg. Sci.* 11: 179-188.

Box, E.O., Holben, B.N. & Kalb, V. 1989. Accuracy of the AVHRR vegetation index as a predictor of biomass, primary productivity and net CO_2 flux. *Vegetatio* 80: 71-89.

Burke, I.C., Lauenroth, W.K. & Parton, W.J. 1997. Regional and temporal variability in aboveground net primary productivity and net N mineralization in grasslands. *Ecology* 78: 1330-1340.

Coops, N.C. & Waring, R.H. 2001. Assessing forest growth across southwestern Oregon under a range of current and future global change scenarios using a process model, 3-PG. *Glob. Change Biol.* 7: 15-29.

Curtis, P.S., Hanson, P.J., Bolstad, P., Barford, C., Randolph, J.C., Schmid, H.P. & Wilson, K.B. 2002. Biometric and eddy-covariance based estimates of annual carbon storage in five eastern North American deciduous forests. *Agric. For. Meteor.* 113: 3-19.

Di Bella, C.M., Rebella, C.M. & Paruelo, J.M. 2000. Evapotranspiration estimates using NOAA AVHRR imagery in the Pampa region of Argentina. *Int. J. Remote Sens.* 21: 791-797.

Field, C.B., Randerson, J.T. & Malmström, C.M. 1995. Global net primary production: combining ecology and remote sensing. *Remote Sens. Environ.* 51: 74-88.

Goetz, S.J. & Prince, S.D. 1999. Modelling terrestrial carbon exchange and storage: evidence and implications of functional convergence in light-use efficiency. *Adv. Ecol. Res.* 28: 57-92.

Hueck, K. & Seibert, P. 1981. *Vegetationskarte von Südamerika*. Fischer Verlag, Stuttgart, DE.

James, M.E. & Kalluri, S.N.V. 1994. The Pathfinder AVHRR land data set: an improved coarse resolution data set for terrestrial monitoring. *Int. J. Remote Sens.* 15: 3347-3363.

Kaufman, Y.J. & Holben, B.N. 1993. Calibration of the AVHRR visible and near-IR bands by atmospheric scattering, ocean glint, and desert reflection. *Int. J. Remote Sens.* 14: 21-52.

Leemans, R. & van den Born, J. 1994. Determining the potential distribution of vegetation, crops and agricultural productivity. *Water Air Soil Poll.* 76: 133-161.

McNaughton, S.J., Oesterheld, M., Frank, D.A. & Williams, K.J. 1989. Ecosystem-level patterns of primary productivity and herbivory in terrestrial habitats. *Nature* 341: 142-144.

McNaughton, S.J., Sala, O.E. & Oesterheld, M. 1993. Comparative ecology of African and South American arid to subhumid ecosystems. In: Goldblatt, P. (ed.) *Biological relationships between Africa and South America*, pp. 548-567. Yale University Press. New Haven, CT, US.

Milchunas, D.G. & Lauenroth, W.K. 1992. Carbon dynamics and estimates of primary production by harvest, ^{14}C dilution and ^{14}C turnover. *Ecology* 73: 593-607.

Monteith, J.L. 1981. Climatic variation and the growth of crops. *Q. J. R. Meteor. Soc.* 107: 749-774.

Moran, M.S., Clarke, T.R., Inoue, Y. & Vidal, A. 1994. Estimating crop water deficit using the relation between surface-air temperature and spectral vegetation index. *Remote Sens. Environ.* 49: 246-263.

Nemani, R. & Running, S. 1997. Land cover characterization using multitemporal red, near-IR, and thermal-IR data from NOAA/AVHRR. *Ecol. Appl.* 7: 79-90.

Noy-Meir, I. 1973. Desert ecosystems: Environments and producers. *Annu. Rev. Ecol. Syst.* 4: 25-51.

Oesterheld, M., Sala, O.E. & McNaughton, S.J. 1992. Effect of animal husbandry on herbivore-carrying capacity at a regional scale. *Nature* 356: 234-236.

Paruelo, J.M. & Lauenroth, W.K. 1995. Regional patterns of NDVI in North American shrublands and grasslands. *Ecology* 76: 1888-1898.

Paruelo, J.M. & Lauenroth, W.K. 1998. Interannual variability

of the NDVI curves and their climatic controls in North American shrublands and grasslands. *J. Biogeogr.* 25: 721-733.

Paruelo, J.M., Jobbagy, E.G., Sala, O.E., Lauenroth, W.K. & Burke, I.C. 1998. Functional and structural convergence of temperate grassland and shrubland ecosystems. *Ecol. Appl.* 8: 194-206.

Paruelo, J.M., Lauenroth, W.K., Burke, I.C. & Sala, O.E. 1999. Grassland precipitation-use efficiency varies across a resource gradient. *Ecosystems* 2: 64-68.

Potter, C.S, Klooster, S. & Brooks, V. 1999. Interannual variability in terrestrial net primary production: exploration of trends and controls on regional to global scales. *Ecosystems* 2: 36-48.

Prentice, I.C., Cramer, W., Harrison, S.P., Leemans, R., Monserud, R.A. & Solomon, A.M. 1992. A global biome model based on plant physiology and dominance, soil properties and climate. *J. Biogeogr.* 19: 117-134.

Pucheta, E., Cabido, M., Díaz, S. & Funes, G. 1998. Floristic composition, biomass, and aboveground net plant production in grazed and protected sites in a mountain grassland of central Argentina. *Acta Oecol.* 19: 97-105.

Running, S.W. & Nemani, R.R. 1988. Relating seasonal patterns of the AVHRR vegetation index to simulated photosynthesis and transpiration of forests in different climates. *Remote Sens. Environ.* 24: 347-367.

Sala, O.E, Parton, W.J., Joyce, L.A. & Lauenroth, W.K. 1988. Primary production of the central grassland region of the United States. *Ecology* 69: 40-45.

Saxton, K.E., Rawls, W.J., Romberger, J. & Papendick,R. 1986. Estimating generalized soil-water characteristics from texture. *Soil Sci. Soc. Am. J.* 50: 1031-1036.

Schultz, P.A. & Halpert, M.S. 1995. Global analysis of the relationships among a vegetation index, precipitation and land surface temperature. *Int. J. Remote Sens.* 16: 2755-2777.

Sobrino, J.A., Coll, C. & Caselles, V. 1991. Atmospheric correction for land surface temperature using NOAA-11 AVHRR Channels 4 and 5. *Remote Sens. Environ.* 38: 19-34.

Stephenson, N.L. 1990. Climatic control of vegetation distribution: the role of the water balance. *Am. Nat.* 135: 649-670.

Tucker, C.J. & Sellers, P.J. 1986. Satellite remote sensing for primary production. *Int. J. Remote Sens.* 7: 1395-1416.

Tüxen, R. 1956. Die heutige potentielle natürliche Vegetation als Gegenstand der Vegetationskartierung. *Angew. Pflanzensoziol.* (Stolzenau) 13: 4-42.

Veblen, T.T., Donoso, C., Kitzberger, T. & Rebertus, A.J. 1996. Ecology of Southern Chilean and Argentinean *Nothofagus* forests. In: Veblen, T.T., Hill, R.S. & Read, J. (eds.) *The ecology and biogeography of Nothofagus forests*. Yale University Press, New Haven, CT, US.

Viovy, N., Arino, O. & Belward, A.S. 1992. The Best Index Slope Extraction (BISE): A method for reducing noise in NDVI time-series. *Int. J. Remote Sens.* 13: 1585-1590.

Wright, S.J. 1996. Plant species diversity and ecosystem functioning in tropical forest. In: Orians, G.H., Dirzo, R. & Cushman, J.H. (eds.) *Biodiversity and ecosystem processes in tropical forests*. Springer, Berlin, DE.

Received 29 April 2003;
Accepted 28 June 2004.
Co-ordinating Editor: K. Woods.

For Apps. 1-3, see JVS/AVS Electronic Archives; www.opuluspress.se/pub/archives/index.htm